

obtain

Crystal Structure and Luminescence of a Europium Coordination Polymer $\{[\text{Eu}(p\text{-MOBA})_3 \cdot 2\text{H}_2\text{O}] \cdot 0.5\text{H}_2\text{O} \cdot 0.5(4,4'\text{-bipy})\} \infty$

LI, Xia^{a,b} (李夏) JIN, Lin-Pei^{*a} (金林培) WAN, Yong-Hong^a (王永红)
 LU, Shao-Zhe^c (吕少哲) ZHANG, Jia-Hua^c (张家骅)

^a Department of Chemistry, Beijing Normal University, Beijing 100875, China

^b Department of Chemistry, Capital Normal University, Beijing 100037, China

^c Laboratory of Excited State Processes, Chinese Academy of Sciences, Changchun, Jilin 130021, China

The structure of the complex $\{[\text{Eu}(p\text{-MOBA})_3 \cdot 2\text{H}_2\text{O}] \cdot 0.5\text{H}_2\text{O} \cdot 0.5(4,4'\text{-bipy})\} \infty$ (*p*-MOBA: *p*-methoxybenzoate, 4,4'-bipy: 4,4'-bipyridine) was determined by single crystal X-ray diffraction study. Each europium atom is coordinated with two oxygen atoms of the chelated carboxyl group, four oxygen atoms of the four bidentate bridging carboxylate groups and two oxygen atoms of two water molecules, forming an infinite polymeric chain structure. Excitation and luminescence spectra were observed at 77 K. The high resolution spectrum of the complex shows that the europium ion site in the crystal has low symmetry. The complex displays intense luminescence which may be related to the *p*-MOBA ligand and the polymeric coordination.

Keywords europium *p*-methoxybenzoate dihydrate, X-ray crystallography, luminescence

Introduction

Mononuclear, dinuclear and polymeric types of crystal structures for lanthanide complexes with benzoic acid and its derivatives have been obtained because of the variation of bridging forms for carboxylate group and coordination ability of diamine ligands, such as 1,10-phenanthroline, 2,2'-bipyridine and 4,4'-bipyridine.¹⁻³ In the crystal structures of the lanthanide coordination polymers the bidentate and the tridentate bridging modes of the car-

boxyl group are commonly found.³⁻⁵ Europium luminescent probe has been widely used in local structure determination of crystalline materials.⁶ Our interest focuses on the study of crystal structures of europium complexes and their high-resolution, laser-excited excitation and emission spectra.⁷⁻¹⁰ As part of a series of our study on crystal structure and luminescence of lanthanide carboxylate complexes we report here the results of an X-ray diffraction analysis for the europium coordination polymer $\{[\text{Eu}(p\text{-MOBA})_3 \cdot 2\text{H}_2\text{O}] \cdot 0.5\text{H}_2\text{O} \cdot 0.5(4,4'\text{-bipy})\} \infty$ (*p*-MOBA: *p*-methoxybenzoate, 4,4'-bipy: 4,4'-bipyridine) and its luminescence property.

Experimental

Preparation

0.35 mmol of $\text{Eu}(\text{NO}_3)_3 \cdot 6\text{H}_2\text{O}$, 1.2 mmol of *p*-MOBA and 0.4 mmol of 4,4'-bipyridine were dissolved in 25 mL of mixed solvent of ethanol and water (ethanol: $\text{H}_2\text{O} = 2:1$, V/V). The pH of the solution was adjusted to ~ 5.0 with 2 mol/L NaOH solution. The mixed solution was stirred for 5 h at 60–70 °C. A white precipitate was formed. Crystals of $\{[\text{Eu}(p\text{-MOBA})_3 \cdot 2\text{H}_2\text{O}] \cdot 0.5\text{H}_2\text{O} \cdot 0.5(4,4'\text{-bipy})\} \infty$ suitable for X-ray analysis were

* E-mail: ljin@bnu.edu.cn

Received June 26, 2001; revised and accepted November 13, 2001.

Project supported by State Key Project of Fundamental Research (No. G1998061308), the National Natural Science Foundation of China (No. 29971005) and Natural Science Foundation of Beijing (No. 2982009).

X-ray

0.20

data v

20.0

value

larizat

used.

nique

Patter

drogen

liabili

|F_o|

where

using

crysta

Form

Crys

Wav

Crys

Lati

Volu

Spac

Z

D_c

F(0

Absc

Tem

2θ_{min}

Refl

Inde

Refl

Inde

Date

R,

Goo

Larg

obtained from the mother liquor after 20 days.

X-ray structure determination

A colorless prismatic crystal with dimensions $0.20 \times 0.20 \times 0.30 \text{ mm}^3$ was mounted on a glass fibre. Intensity data were collected on a Rigaku AFC7R diffractometer at 20.0°C using the ω - 2θ scan technique to a maximum 2θ value of 50.9° . Data were corrected for Lorentz and polarization effects. Empirical absorption corrections were used. Of the 4659 collected reflections, 4378 were unique ($R_{\text{int}} = 0.044$). The structure was solved by the Patterson method and refined anisotropically for non-hydrogen atom by full-matrix least-squares calculations. Reliability factors are defined as $R = \sum(|F_o| - |F_c|) / \sum |F_o|$ and $R_w = \{ \sum w(|F_o| - |F_c|)^2 / \sum |F_o|^2 \}^{1/2}$ where $w = 4F_o^2 / \sigma^2(F_o^2)$. All calculations were performed using TEXSAN crystallographic software package.¹¹ The crystal data and experimental details are given in Table 1.

Table 1 The crystal data and experimental details

Formula weight	1457.03
Crystal size	$0.20 \times 0.20 \times 0.30 \text{ mm}^3$
Wavelength (Mo K α)	0.071069 nm
Crystal system	triclinic
Lattice parameters	$a = 1.2768(4) \text{ nm}$, $\alpha = 94.29(3)^\circ$ $b = 1.3735(5) \text{ nm}$, $\beta = 94.51(2)^\circ$ $c = 0.9607(2) \text{ nm}$, $\gamma = 114.47(3)^\circ$
Volume	$1.5533(10) \text{ nm}^3$
Space group	$P\bar{1}$
Z	1
D_c	1.56 g/cm^3
$F(000)$	732.00
Absorption coefficient	20.7 mm^{-1}
Temperature	$273 \pm 1^\circ \text{C}$
$2\theta_{\text{max}}$	50.9°
Reflections collected	4659
Independent reflections	4378 [$R_{\text{int}} = 0.044$]
Refinement method	Full-matrix least-squares on F^2
Index ranges	$0 \leq h \leq 13$, $-16 \leq k \leq 15$, $-11 \leq l \leq 11$
Data/restraints/parameters	4378/0/383
R , R_w	0.036, 0.047
Goodness of fit indicator	1.62
Largest diff. peak and hole	1110 e/nm^3 and -830 e/nm^3

Excitation and emission spectral measurements

The excitation and luminescence spectra for the crystals of complex were recorded with YAG:Nd³⁺ laser using Spex1403 double grating monochromator. High-resolution spectrum was recorded at 77 K using PLT-2000 laser (Rhodamine 6G) pumped by N₂ laser.

Results and discussion

Structure of $\{ [\text{Eu}(p\text{-MOBA})_3 \cdot 2\text{H}_2\text{O}] \cdot 0.5 \text{H}_2\text{O} \cdot 0.5(4,4'\text{-bipy}) \}_\infty$

A fragment of the structure of the title complex is shown in Fig. 1, where can be seen that each Eu³⁺ ion is bonded to two oxygen atoms of the chelating carboxylate group and two oxygen atoms of two water molecules, and coordinates with four bidentate bridging carboxyl groups which link two neighboring Eu³⁺ ions forming an infinite polymeric chain. A projection of the packing of the title complex along the axis a is shown in Fig. 2, from which it can be seen that there are channels between the chains and the 4,4'-bipy molecules distribute over them. The nitrogen atoms of the 4,4'-bipy molecules form hydrogen bonds with the bonded waters, which contribute to the stability of the title compound. This is unlike the complex $[\text{Eu}(p\text{-MOBA})_3 \cdot 2,2'\text{-bipy}]$ (2,2'-bipy: 2,2'-bipyridine) in which the two europium ions are linked by the bridging carboxylate groups to form a dinuclear europium complex² and 2,2'-bipy is chelated to the Eu³⁺ ion since 2,2'-bipy is likely to form a chelated ring, but 4,4'-bipy is not involved in coordination for the title complex. It is also unlike the complex of Eu(DBM)₃ (4,4'-bipy) (DBM: dibenzoylmethanato)⁹ in which 4,4'-bipy is bonded to the two neighbouring europium ions to form an infinite polymeric chain. This is because the β -diketone ligand generally acts as the chelating one in lanthanide β -diketone complexes and the bridging mode is rarely found.¹²

The atomic coordinates and thermal parameters, selected bond lengths and bond angles are listed in Tables 2–3, respectively. The average distance of Eu—O (the chelated carboxyl group) is 0.2486 nm and that of Eu—O (the bridging carboxyl group) is 0.2350 nm (Table 2). This indicates that the former Eu—O distance is longer than the latter one, which clearly shows that formation of four-membered ring for the carboxylate group

dina-
t, 4'-

ninescent
determina-
s on the
and their
emission
n crystal
late com-
iffraction
[Eu(*p*-
(*p*-MO-
pyridine)

sol of *p*-
dissolved
ethanol:
adjusted
red solu-
recipitate
0] · 0.5
ysis were

undation of

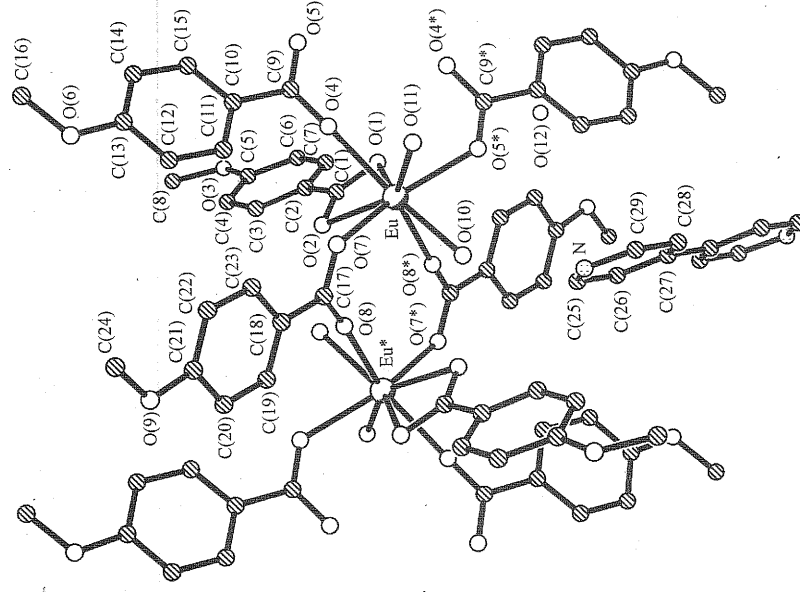


Fig. 1 Molecular structure of $[\{\text{Eu}(p\text{-MOBA})_3 \cdot 2\text{H}_2\text{O}\}] \cdot 0.5\text{H}_2\text{O} \cdot 0.5(4,4'\text{-bipy})_\infty$ (H atoms have been omitted for clarity).

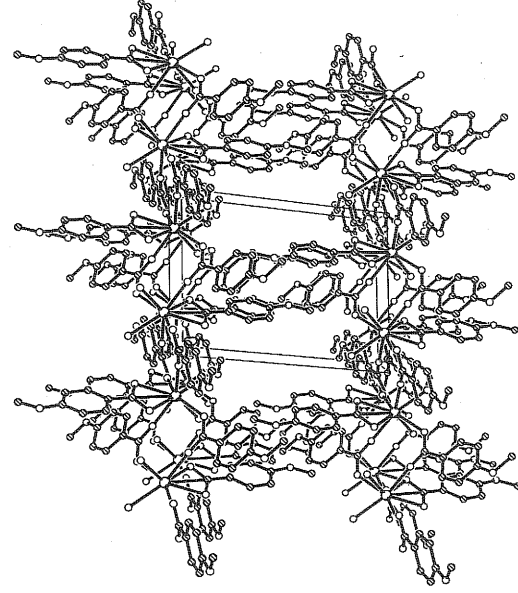


Fig. 2 Packing of the title complex viewed along the axis *a* (Unbonded water molecules, 4,4'-bipy molecules and H atoms have been omitted for clarity).

Table 2 Non-hydrogen atomic coordinates and thermal parameters $B(\text{eq})$

Atom	<i>x</i>	<i>y</i>	<i>z</i>	$B(\text{eq})$ ($\times 10^3 \text{ nm}^2$)
Eu	-0.01191(3)	0.02340(2)	-0.24511(3)	2.098(8)
O(1)	0.0990(4)	-0.0817(3)	-0.3312(5)	2.9(1)
O(2)	-0.0301(4)	-0.1547(3)	-0.1922(5)	2.9(1)
O(3)	0.1297(6)	-0.5317(4)	-0.3592(7)	5.7(2)
O(4)	-0.1196(4)	-0.0849(4)	-0.4440(5)	3.3(1)
O(5*)	-0.1332(4)	-0.1536(3)	-0.6624(5)	3.1(1)
O(6)	-0.6184(4)	-0.4218(5)	-0.5059(7)	6.0(2)
O(7)	-0.1894(4)	-0.0243(4)	-0.1556(5)	3.0(1)
O(8*)	-0.1254(4)	-0.0438(4)	0.0545(5)	3.3(1)
O(9)	-0.6476(4)	-0.1969(6)	0.1212(6)	6.2(2)
O(10)	0.0017(4)	0.1799(3)	-0.0871(4)	2.8(1)
O(11)	-0.1100(4)	0.1187(4)	-0.3797(5)	3.5(1)
O(12)	0.649(2)	0.076(2)	-0.396(2)	11.7(6)
N	0.2013(6)	0.3739(5)	-0.0118(7)	4.7(2)
C(1)	0.0440(6)	-0.1594(5)	-0.2683(7)	2.8(1)
C(2)	0.0676(6)	-0.2580(5)	-0.2854(7)	2.8(2)
C(3)	-0.0072(6)	-0.3501(6)	-0.2480(8)	3.7(2)
C(4)	0.0109(7)	-0.4430(6)	-0.272(1)	4.6(2)
C(5)	0.1043(7)	-0.4432(6)	-0.3315(8)	4.1(2)
C(6)	0.1839(7)	-0.3503(7)	-0.363(1)	4.5(2)
C(7)	0.1637(6)	-0.2588(6)	-0.3427(8)	3.6(2)
C(8)	0.0475(9)	-0.6302(6)	-0.342(1)	5.9(3)
C(9)	-0.1715(5)	-0.1501(5)	-0.5475(6)	2.3(1)
C(10)	-0.2874(5)	-0.2268(5)	-0.5352(7)	2.7(1)
C(11)	-0.3428(6)	-0.2160(6)	-0.4227(8)	4.5(2)
C(12)	-0.4527(7)	-0.2833(7)	-0.416(1)	5.7(2)
C(13)	-0.5093(6)	-0.3623(6)	-0.5219(8)	4.0(2)
C(14)	-0.4552(6)	-0.3747(6)	-0.6344(8)	4.0(2)
C(15)	-0.3447(6)	-0.3074(6)	-0.6393(7)	3.6(2)
C(16)	-0.6835(7)	-0.5021(7)	-0.615(1)	5.6(2)
C(17)	-0.2054(5)	-0.0480(5)	-0.0332(7)	2.4(1)
C(18)	-0.3223(5)	-0.0843(5)	0.0067(7)	2.5(1)
C(19)	-0.3452(6)	-0.1082(7)	0.1396(8)	4.1(2)
C(20)	-0.4532(7)	-0.1461(8)	0.1755(8)	5.0(2)
C(21)	-0.5431(6)	-0.1612(6)	0.075(1)	4.2(2)
C(22)	-0.5246(6)	-0.1376(6)	-0.0600(8)	3.9(2)
C(23)	-0.4141(6)	-0.1003(6)	-0.0925(7)	3.3(2)
C(24)	-0.7441(7)	-0.2130(8)	0.026(1)	6.6(3)
C(25)	0.2702(8)	0.3286(6)	0.029(1)	5.5(2)
C(26)	0.3873(7)	0.3743(6)	0.036(1)	5.2(2)
C(27)	0.4367(6)	0.4739(6)	-0.0024(7)	3.7(2)
C(28)	0.3651(7)	0.5223(7)	-0.042(1)	6.2(3)
C(29)	0.2497(8)	0.4702(8)	-0.044(1)	6.4(3)

parameters

 $B(\text{eq})$
 $\times 10^2 \text{ nm}$

2.098(8)

2.9(1)

2.9(1)

5.7(2)

3.3(1)

3.1(1)

6.0(2)

3.0(1)

3.3(1)

6.2(2)

2.8(1)

3.5(1)

11.7(6)

4.7(2)

2.8(1)

2.8(2)

3.7(2)

4.6(2)

4.1(2)

4.5(2)

3.6(2)

5.9(3)

2.3(1)

2.7(1)

4.5(2)

5.7(2)

4.0(2)

4.0(2)

3.6(2)

5.6(2)

2.4(1)

2.5(1)

4.1(2)

5.0(2)

4.2(2)

3.9(2)

3.3(2)

6.6(3)

5.5(2)

5.2(2)

3.7(2)

6.2(3)

6.4(3)

has larger tension. It is noticed that hydrogen bond is formed between bonded and unbonded water molecules. The distance of O(11)—H(24) is 0.1130 nm and that of the O(12)···H(24) is 0.1831 nm. The O(11)—H(24)···O(12) angle is 156.6°. Furthermore, the oxygen atoms of the bidentate chelating carboxyl group form hydrogen bonds with bonded water molecules, such as O(1)···H(25*)—O(11*) and O(10)—H(23)···O(2). The bond distances of O(1)···H(25*), H(25*)—O(11*), H(23)···O(2) and O(10)—H(23) are 0.187, 0.095, 0.187 and 0.089 nm, respectively. The bond angles of O(1)···H(25*)—O(11*) and O(10)—H(23)···O(2) are 171.6° and 166.7°, respectively. In addition, the distance for the two neighboring europium ion ranges from 0.480 to 0.494 nm. And the bond angle of O(7)—C(17)—O(8) [123.8(6)°] is slightly larger than that of O(4)—C(9)—O(5) [121.6(6)°]. These results show that the environment of Eu^{3+} ions is very similar but not identical.

cal. The calculated results of the least-squares planes show that the europium complex has no stacking effect of aromatic rings as commonly observed in dinuclear europium complexes with benzoic acid and its derivatives.^{3,13}

Luminescence study

The emission spectrum of $\{[\text{Eu}(p\text{-MOBA})_3 \cdot 2\text{H}_2\text{O}] \cdot 0.5\text{H}_2\text{O} \cdot 0.5(4,4'\text{-bipy})\}_\infty$ crystals obtained under excitation of 355 nm is presented in Fig. 3. It almost exclusively contains emission bands from the excited state 5D_0 , and the number of components of the transitions ${}^5D_0 \rightarrow {}^7F_J$ ($J=0-3$) indicates low symmetry of the Eu^{3+} ion site in the complex.⁶ This is in agreement with the results of X-ray analysis for the complex. The transition ${}^5D_0 \rightarrow {}^7F_0$ is particularly weak and was consequently studied by selective excitation technique.

The high-resolution ${}^7F_0 \rightarrow {}^5D_0$ spectra recorded by monitoring at 16193 (a), 16956 (b) and 16809 cm^{-1}

Table 3 selected bond lengths and bond angles for the complex

	distances (nm)		
Eu—O(1)	0.2505(4)	Eu—O(7)	0.2369(4)
Eu—O(2)	0.2466(4)	Eu—O(8*)	0.2359(5)
Eu—O(4)	0.2328(4)	Eu—O(10)	0.2480(4)
Eu—O(5*)	0.2343(4)	Eu—O(11)	0.2481(5)
		angles (°)	
O(1)—Eu—O(2)	52.6(1)	O(4)—Eu—O(7)	83.4(2)
O(1)—Eu—O(4)	73.5(2)	O(4)—Eu—O(8*)	145.5(2)
O(1)—Eu—O(5*)	79.6(2)	O(4)—Eu—O(10)	141.2(2)
O(1)—Eu—O(7)	132.7(2)	O(4)—Eu—O(11)	70.4(2)
O(1)—Eu—O(8*)	75.6(2)	O(5*)—Eu—O(7)	146.9(2)
O(1)—Eu—O(10)	143.5(1)	O(5*)—Eu—O(8*)	85.7(2)
O(1)—Eu—O(11)	129.2(1)	O(5*)—Eu—O(10)	80.3(1)
O(2)—Eu—O(4)	76.3(2)	O(5*)—Eu—O(11)	75.4(2)
O(2)—Eu—O(5*)	130.7(2)	O(7)—Eu—O(8*)	107.2(2)
O(2)—Eu—O(7)	82.4(2)	O(7)—Eu—O(10)	75.0(1)
O(2)—Eu—O(8*)	72.8(2)	O(7)—Eu—O(11)	76.6(2)
O(2)—Eu—O(10)	130.5(1)	O(8*)—Eu—O(10)	72.8(2)
O(2)—Eu—O(11)	142.3(2)	O(8*)—Eu—O(11)	143.5(2)
O(4)—Eu—O(5*)	103.4(2)	O(10)—Eu—O(11)	73.4(1)

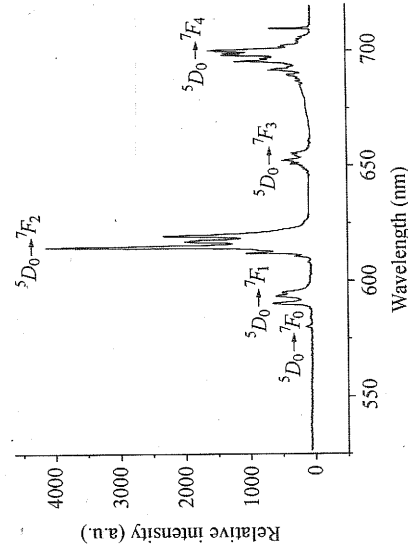


Fig. 3 Luminescence spectrum of $\{[\text{Eu}(p\text{-MOBA})_3 \cdot 2\text{H}_2\text{O}]\}_\infty \cdot 0.5\text{H}_2\text{O} \cdot 0.5(4,4'\text{-bipy})\}_\infty$ at 77 K, $\lambda_{\text{exc}} = 355$ nm.

(c), respectively, are shown in Fig. 4. Each of them displays some shoulders or additional splitting, which is similar to the bipy-containing Eu complexes.^{2,9} However, spectra a, b and c are similar and have comparable line positions. The broadened excitation spectra may be attributed to the Eu^{3+} ions which are involved in slightly different chemical environment as described previously.

The selectively excited emission bands of transition $^5D_0 \rightarrow ^7F_1$ under excitation of 579.40 and 579.70 nm, respectively are given in Fig. 5. Each of them labeled a or b is composed of three main components with some shoulders. The bands shown in Fig. 5a and 5b are attributed to almost identical crystal field splitting for the Eu^{3+} ions, and these will be simply referred to as one Eu^{3+} ion site in the title complex.

The fluorescence kinetics of $\{[\text{Eu}(p\text{-MOBA})_3 \cdot 2\text{H}_2\text{O}] \cdot 0.5\text{H}_2\text{O} \cdot 0.5(4,4'\text{-bipy})\}_\infty$ excited at 579.70 nm and monitored at 16941 cm^{-1} is shown in Fig. 6. The kinetics behavior of $\{[\text{Eu}(p\text{-MOBA})_3 \cdot 2\text{H}_2\text{O}] \cdot 0.5\text{H}_2\text{O} \cdot 0.5(4,4'\text{-bipy})\}_\infty$ fluorescence showed mono-exponentiality. The observed lifetime τ is 0.40 ms. The title complex displays rapid fluorescence decay because water molecules are directly bonded to the Eu^{3+} ion and the water molecule is a quenching agent for Eu^{3+} ion emission. However, the complex has intense red fluorescence because of extensive π system of coordination polymer structure of $\{[\text{Eu}(p\text{-MOBA})_3 \cdot 2\text{H}_2\text{O}] \cdot 0.5\text{H}_2\text{O} \cdot 0.5(4,4'\text{-bipy})\}_\infty$.

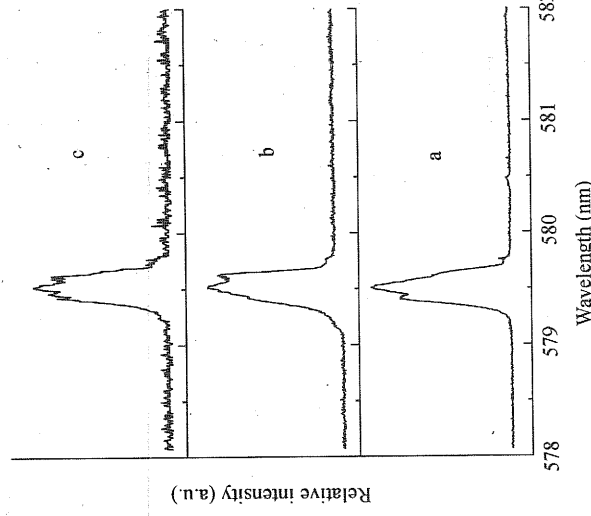


Fig. 4 Excitation spectra of $\{[\text{Eu}(p\text{-MOBA})_3 \cdot 2\text{H}_2\text{O}]\}_\infty \cdot 0.5\text{H}_2\text{O} \cdot 0.5(4,4'\text{-bipy})\}_\infty$ at 77 K. a. $\lambda_{\text{anal.}} = 617.55$ nm, b. $\lambda_{\text{anal.}} = 589.76$ nm, c. $\lambda_{\text{anal.}} = 594.92$ nm.

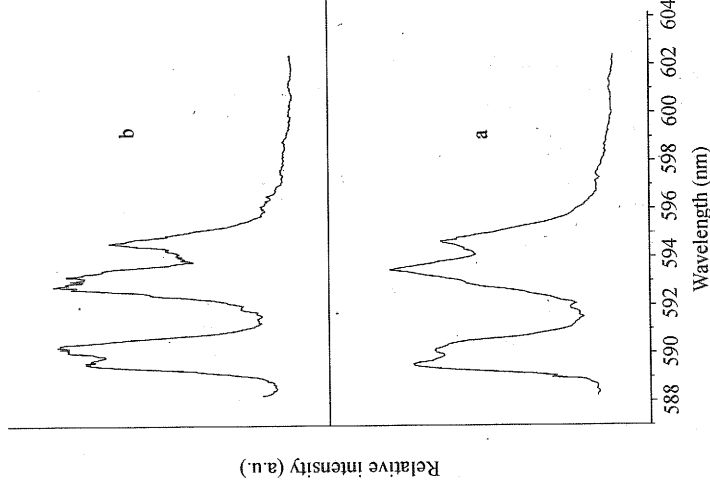


Fig. 5 Emission spectra of $^5D_0 \rightarrow ^7F_1$ transition of $\{[\text{Eu}(p\text{-MOBA})_3 \cdot 2\text{H}_2\text{O}] \cdot 0.5\text{H}_2\text{O} \cdot 0.5(4,4'\text{-bipy})\}_\infty$ at 77 K. a. $\lambda_{\text{ex}} = 579.40$ nm, b. $\lambda_{\text{ex}} = 579.70$ nm.

Ref

17

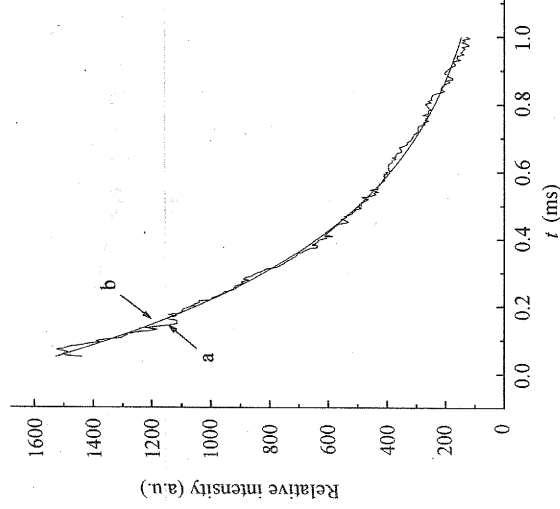


Fig. 6 Decay curve of $[\text{Eu}(p\text{-MOBA})_3 \cdot 2\text{H}_2\text{O}] \cdot 0.5\text{H}_2\text{O} \cdot 0.5(4,4'\text{-bipy}) \}_{\infty}$, at 77 K. a. observed curve, b. fitted curve.

References

- Zheng, X.; Jin, L.; Wang, M. *J. Rare Earths* **1994**, *12*, 248.
- Jin, L.; Wang, R.; Li, L.; Lu, S.; Huang, S. *Polyhedron* **1999**, *18*, 487.
- Li, X.; Zheng, X.; Jin, L.; Lu, S.; Qin, W. *J. Mol. Struct.* **2000**, *519*, 85.
- Ma, J.; Jin, Z.; Ni, J. *Acta Chim. Sin.* **1993**, *51*, 265.
- Ma, J.; Jin, Z.; Ni, J. *Acta Cryst.* **1994**, *C50*, 1008.
- Bünzli, J. C. G.; Choppin, G. R. *Lanthanide Probes in Life, Chemical and Earth Sciences*, Elsevier, Amsterdam, **1989**, Chapter 7.
- Jin, L.; Wang, M.; Cai, G.; Liu, S.; Huang, J.; Wang, R. *Sci. China (Series B)* **1995**, *38*, 1.
- Wang, M.; Jin, L.; Liu, S.; Cai, G.; Huang, J.; Qin, W.; Huang, S. *Sci. China (Series B)* **1994**, *37*, 410.
- Wang, M.; Jin, L.; Wang, Z.; Cai, G.; Zhang, J. *Sci. China (Series B)* **1995**, *38*, 1061.
- Wang, R.; Li, L.; Jin, L.; Lu, S.; Zhang, J. *J. Coord. Chem.* **1999**, *47*, 279.
- TEXSAN; *Crystal Structure Analysis Package*, Molecular Structure Corporation, **1985&1992**.
- Boeyens, J. C. A.; De Villies, J. P. *J. Cryst. Mol. Struct.* **1972**, *2*, 197.
- Zhang, Y.; Jin, L.; Lu, S. *J. Chin. Rare Earth Soc.* **1998**, *16*, 5 (in Chinese).

i. Zheng, X.; Jin, L.; Wang, M. *J. Rare Earths* **1994**,

(E0106266FZ HUANG, W. Q.)